Science of the Total Environment 750 (2021) 141525

Contents lists available at ScienceDirect

Science of the Total Environment

journal homepage: www.elsevier.com/locate/scitotenv

Response of the weathering carbon sink in terrestrial rocks to climate variables and ecological restoration in China

Suhua Gong [a,c,d], Shijie Wang [a,d], Xiaoyong Bai [a,b,e,*], Guangjie Luo [f], Luhua Wu [a,c,d], Fei Chen [a,d,f], Qinghuan Qian [a,d,f], Jianyong Xiao [a,d,f], Cheng Zeng [a,d,f]

[a] State Key Laboratory of Environmental Geochemistry, Institute of Geochemistry, Chinese Academy of Sciences, Guiyang 550081, Guizhou Province, China
[b] CAS Center for Excellence in Quaternary Science and Global Change, Xi'an 710061, Shanxi Province, China
[c] University of Chinese Academy of Sciences, Beijing 100049, China
[d] Puding Karst Ecosystem Observation and Research Station, Chinese Academy of Sciences, Puding 562100, Guizhou Province, China
[e] Guizhou Provincial Key Laboratory of Geographic State Monitoring of Watershed, Guizhou Education University, Guiyang 550018, China
[f] School of Geography and Environmental Sciences, Guizhou Normal University, Guiyang 550001, China

HIGHLIGHTS

- High sensitivity of the CSF to climate change and ecological restoration.
- Water budget and precipitation are the main factors affecting the change in the CSF.
- The CSF in China showed a decreasing trend.
- Mixed sedimentary rocks and the Pearl River Basin have the highest CSF, respectively.
- Spatiotemporal distribution and dynamic change of the CSF.

GRAPHICAL ABSTRACT

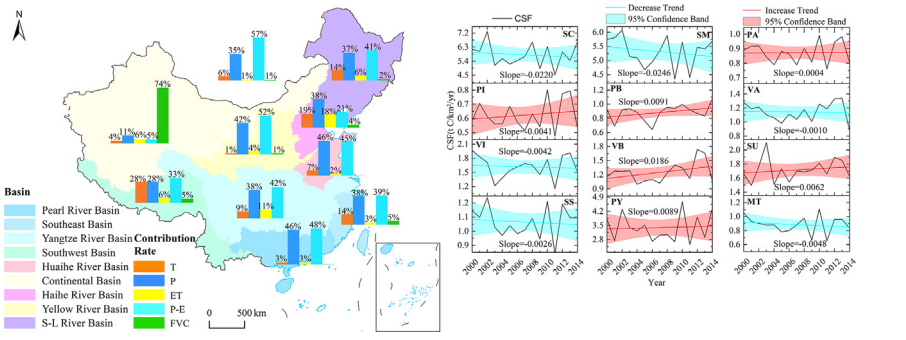

ARTICLE INFO

Article history:
Received 8 November 2019
Received in revised form 18 July 2020
Accepted 4 August 2020
Available online 4 August 2020

Editor: Ouyang Wei

Keywords:
Carbon sink
Rock
Climate change
Ecological restoration
GEM-CO_2

ABSTRACT

The weathering carbon sink (CS) of rocks has a sensitive response to different influencing factors, and it is important to accurately distinguish this response in the global carbon cycle. However, no quantitative analysis of the response mechanism has been performed. In this study, the CS of the 12 types of terrestrial rocks in China from 2000 to 2014 is estimated using the GEM-CO_2 model. The relative contribution rates of climate change and ecological restoration to the CS are quantitatively evaluated using the Lindeman-Merenda-Gold model. Results showed that: (1) The CS of terrestrial rocks in China was 17.69 Tg C yr^{-1}, and the CS flux (CSF) was 2.53 t C km^{-2} yr^{-1}; mixed sedimentary rocks had the highest CS (6.89 Tg C yr^{-1}), and carbonate rocks had the highest CSF (5.8 t C km^{-2} yr^{-1}). (2) The average annual CSF slightly decreased at a rate of 5.4 kg C km^{-2} yr^{-1}; the areas of the CSF that decreased in the south were the areas where water budget decreased significantly, and it was the areas with a reduced water budget and ecological deterioration in the north. (3) The relative contribution rates of water budget and precipitation reached 57% and 35%, respectively; the response of the CSF to temperature was evident in areas with low or decreasing temperatures, and the influence of fractional vegetation cover (FVC) on the CSF in low value area was evident. (4) Mixed sedimentary rocks and carbonate rocks displayed a more evident reduction trend in the CSF than other rocks. This research verified the applicability of the GEM-CO_2 model in China and presented a scientific basis for quantitative assessment of the impact of climate change and ecological restoration on the CSF.

* Corresponding author at: State Key Laboratory of Environmental Geochemistry, Institute of Geochemistry, Chinese Academy of Sciences, Guiyang 550081, Guizhou Province, China.
E-mail address: baixiaoyong@126.com (X. Bai).

https://doi.org/10.1016/j.scitotenv.2020.141525
0048-9697/

1. Introduction

The increase in atmospheric carbon dioxide (CO_2) has an important impact on the greenhouse effect. It is expected to not only affect global climate change but also cause serious environmental disasters (Leighton, 2011; Burton-Chellew et al., 2013). Therefore, the global carbon cycle has become a trending topic in global change research. A key issue in the current carbon cycle research indicates that the carbon sink (CS) do not balance with the carbon source, and the number of "missing CS" is large (Schimel, 1995; Kheshgi et al., 1996; Kennedy, 2001). From observations of ground vegetation, monitoring of atmospheric CO_2/O_2 concentration, information of satellite remote sensing, and simulations of ecological/atmospheric models, researchers have suggested that the mid-high latitude terrestrial ecosystems of the Northern Hemisphere are a significant CS (Schimel et al., 2001; Steven, 2001). Rock weathering exchanges carbon with the atmosphere to consume CO_2 in the atmosphere/soil, and it participates in the short-term and long-term global carbon cycle. The study of the mechanism and influencing factors of the rock CS is crucial to carbon cycle studies. It can not only partially solve the missing CS problem but also contribute to improving carbon cycle models.

At the global scale, researchers, such as Gaillardet (Gaillardet et al., 1999), Gombert (Gombert, 2002), Liu (Liu et al., 2010), and Martin (Martin, 2016), have calculated the carbonate CS using different methods. In China, Qiu used the GEM-CO_2 model to estimate the weathering CS of rocks and their spatial distribution (Qiu et al., 2004). Liu and Zhao estimated the magnitude of the rock CS in China using the hydrochem-discharge and carbonate-rock-tablet-test methods and the diffusion boundary layer (DBL) model (Liu and Zhao, 2000). Li also estimated the magnitude and distribution of the carbonate CS in China using the maximum potential dissolution method (Li et al., 2019a). Researchers have also studied the rock CS in the Pearl River, the Yangtze River, and other river basins (Li and Zhang, 2003; Qin et al., 2013; Fan et al., 2014; Zhang et al., 2016; Liu and Han, 2020).

On the premise of the remarkable research results performed by other researchers, most of the current studies have focused on the carbon consumption of carbonate rocks and silicate rocks weathering (Gaillardet et al., 1999; Amiotte et al., 2003). Furthermore, previous studies have considered the distribution pattern, but have not been involved in its evolution characteristics. In addition, the limitations of the existing methods complicate the large-scale application of the hydrochem-discharge and carbonate-rock-tablet-test methods at the national or global scales. With the worsening of global climate change, people have explored and analyzed the response mechanism of the rock CS on climate change and ecological restoration. Generally, the increase in global temperature will affect the hydrologic cycle by changing precipitation and fractional vegetation cover (FVC), and this will subsequently affect chemical weathering of terrestrial rocks. Therefore, the weathering carbon sink flux (CSF) is potentially sensitive to ongoing climate and land-use changes (Post et al., 1992; Beaulieu et al., 2012). Although some researchers have studied the impact of climate change and other factors on the weathering CS of rocks, the relative contribution rates of influencing factors have not been quantified to determine the different responses of the rock CS to various influencing factors. Therefore, the recent quantifications of the weathering CS of rocks must be re-estimated, and the response of the CS on climate change and ecological restoration must be qualitatively and quantitatively explored and analyzed.

In this study, the Lindeman-Merenda-Gold (LMG) model is used to quantitatively evaluate the response mechanism of the rock CS to climate change and ecological restoration in China from 2000 to 2014. The objectives of this study are presented as follows: (1) to calculate the magnitude and flux of the terrestrial rock CS in China and explore the differences in the CSF from lithologies in the different basins based on the GEM-CO_2 model; (2) to analyze the spatiotemporal distribution and dynamic changes of the CSF and its influencing factors; (3) to quantify the relative contribution rates of various factors that affect the CSF and to explore the main controlling factors and the response mechanism of the CSF evolution; (4) to discriminate the temporal evolution characteristics of different lithologic CSFs and their sensitivity to various impact factors, and to analyze the similarities and differences in the relative contribution rates of different lithologies and influencing factors.

2. Data and methods

2.1. Data

In this study, temperature (Gaillardet et al., 2018; Romero-Mujalli and Hartmann, 2018), precipitation (Zeng C et al., 2016; Zeng S et al., 2016), evapotranspiration, and water budget were selected as the indicators of climate change. The daily maximum and minimum temperature data were derived from the global daily temperature datasets provided by the Climate Prediction Center of the National Oceanic and Atmospheric Administration (NOAA CPC) with a spatial resolution of 0.5°. The daily total precipitation data were analyzed from Global Unified Gauge-Based Analysis of Daily Precipitation dataset with a resolution of 0.5°. The evapotranspiration data were collected from the monthly evapotranspiration datasets with a resolution of 0.25° in the GLDAS 2.1 Noah dataset from the Goddard Earth Sciences Data and Information Services Center (GES DISC). The GLDAS data combine satellite and ground-based observations and utilize the land surface model (LSM) and the technology of data assimilating to provide multiple types of high quality datasets. FVC was chosen as the standard for quantifying the ecological restoration effects (Fang et al., 2001; Fang et al., 2014). It was derived from the global 1 km-resolution of 10-day FVC product provided by the Copernicus Global Land Service supported by the European Commission's Earth Observation Programme. Considering the availability of the data and the accuracy of the results, the above data were selected for the study period (2000–2014). The lithology map of China was obtained from the PANGAEA database with a resolution of 0.5°, and the watershed map was derived from the Resource and Environment Data Cloud Platform.

The monthly and annual average temperatures were collected using the daily minimum and maximum temperature raster data. The annual total precipitation and evapotranspiration were calculated using the daily precipitation and monthly evapotranspiration, respectively. Ignoring the influence of surface runoff and underground runoff on water budget, the water budget data were computed as the difference between the precipitation and evapotranspiration data. The magnitude reflected the extent of water budget and the degree of dry and wet climate (Liu and Zhao, 2000; Cao et al., 2011; Gao and Xu, 2015). All of the data were resampled to the same spatial resolution (0.5°) using the data assimilation model.

2.2. Methods

2.2.1. GEM-CO_2 model

Amiotte and Probst reported that the amount of CO_2 consumed by rock weathering is influenced by rock surface water flow, atmospheric temperature, and rock types (Probst et al., 1992; Amiotte and Probst, 1993). To estimate the amount of carbon consumed by rock weathering and the weathering speed of terrestrial rocks, these authors analyzed the surface runoff and river water chemistry data published by Meybeck (Meybeck, 1979; Meybeck, 1987) for 232 mono-lithologic drainage basins among France. They also established a model to estimate the magnitude of atmospheric CO_2 consumed by weathering of all types of natural rocks. This model is a major achievement of the International Geological Contrast Project 404, and it has been widely popularized and verified in Europe, South America, and Africa. Its formula is expressed as follows:

$$F_{CO_2} = a \times Q \tag{1}$$

where F_{CO_2} is the consumption of CO_2 (mmol km^{-2} s^{-1}); Q is the water flow on the rock surface (l km^{-2} s^{-1}), which is the difference between

precipitation and evapotranspiration; a is the empirical coefficient, which varies by rock types.

2.2.2. Trend analysis method

The regression trend analysis method was used to analyze the spatial evolution trend of the CSF and its influencing factors in China from 2000 to 2014. The calculated gradient reflects the evolution of the CS, where a gradient greater than zero indicates that the pixel has an increasing value during the study period, and the reverse is a decline trend. The magnitude of the gradient reflects the intensity of the increase or decrease in the value of a pixel. A large absolute gradient value indicates a high degree of change. The formula of the gradient is presented as follows (Zhang et al., 2014):

$$\theta = \frac{n \times \sum_{i=1}^{n}(i \times CSF_i) - \left(\sum_{i=1}^{n} i\right)\left(\sum_{i=1}^{n} CSF_i\right)}{n \times \sum_{i=1}^{n} i^2 - \left(\sum_{i=1}^{n} i\right)^2} \quad (2)$$

where θ is the change trend, i is the current year, n is the study period, and CSF_i is the weathering CS of rocks in year i.

2.2.3. Relative contribution rate and correlation evaluation

To evaluate the response index of the weathering CS to various factors in China, the LMG model was used to quantitatively assess the relative importance of climate hydrology and ecological restoration factors to the weathering CS of rocks. The relative importance refers to quantifying the contribution of individual regression factors to multiple regression models. The relative contribution rates of each factor to the CSF in the model were then calculated by averaging all of the possible marginal contributions to the variables and by decomposing the dependent variable variance. Finally, the Pearson coefficient correlation was used to evaluate the correlation between the CSF and its factors. The LMG formula is defined as follows (Sen et al., 1981; Ulrike, 2006):

$$LMG(x_j) = \frac{1}{p}\sum_{k=0}^{p-1} \sum_{\substack{S \subseteq \{x_1,\ldots,x_p\}/\{x_j\} \\ n(S)=k}} \frac{seqR^2(\{x_j\}|S)}{C_{p-1}^{k}} \quad (3)$$

where x is the regression variable, S is the set of variables that were entered into the model, and R^2 is the goodness of fit of model. Therefore, the *LMG* is the expectation of the marginal contribution of regression variable x_j in all sequences.

3. Results

3.1. Spatial distribution of the rock CSF and its impact factors

3.1.1. Magnitude of weathering CSFs in the different basins

The distribution characteristics of rock *CSFs* in each basin were analyzed using the difference in the CO_2 consumption of various types of rocks in the different basins (Table 1). The average annual magnitude of the rock CS in China during 2000–2014 was 17.69 Tg C yr^{-1}; the CSF was 2.53 t C km^{-2} yr^{-1}. During the study period, mixed sedimentary rocks (6.89 Tg C yr^{-1}) and carbonate rocks (4.42 Tg C yr^{-1}) had a higher CS than other rocks. The area of both rocks accounted for 18% and 10% of China's rock distribution, respectively. Their CSs accounted for 39% and 25% of the national CS. Their CSFs were 2.1 and 2.29 times that of the national CSF. Among the nine major river basins, the CSF of the Pearl River Basin (5.96 t C km^{-2} yr^{-1}) was the highest, and the CSF of the Songhua-Liaohe River Basin (0.83 t C km^{-2} yr^{-1}) was the lowest, with a difference of approximately seven times. The Southeast Basin, the Yangtze River Basin, and the Southwest Basin had high CSFs. The type of rock in the different basins with the highest CSF was carbonate rocks. Therefore, exposed lithologies significantly influenced the magnitude of the weathering CS of rocks. The CSF of the basins was greater in the southern regions than in the northern regions, and the

Table 1
Carbon sink fluxes in different basins and rocks.

Regions		Carbonate rocks	Mixed sedimentary rocks	Acid plutonic rocks	Intermediate plutonic	Basic plutonic rocks	Acid volcanic rocks	Intermediate volcanic	Basic volcanic rocks	Unconsolidated sediments	Siliciclastic sediments rocks	Pyroclastic	Metamorphic rocks	CSF
Basins	Pearl River Basin	8.79	9.49	2.25	5.07	N/A	3.46	1.14	4.75	5.40	1.92	N/A	1.58	5.96
	Southeast Basin	11.59	11.93	1.31	N/A	N/A	2.61	4.50	5.17	5.86	2.56	1.94	1.99	4.03
	Yangtze River Basin	6.62	6.66	1.38	1.15	1.61	2.29	5.08	3.64	3.51	1.42	5.97	1.00	4.01
	Southwest Basin	6.02	6.28	1.43	0.46	0.16	2.87	2.97	0.74	2.75	1.44	N/A	1.49	3.76
	Huaihe River Basin	6.44	3.85	0.73	0.35	N/A	N/A	0.42	N/A	2.63	0.95	N/A	0.46	2.02
	Continental Basin	3.59	3.23	0.41	0.51	1.03	0.99	0.75	0.72	0.75	0.60	0.08	0.26	1.64
	Haihe River Basin	2.62	2.47	0.33	N/A	0.22	0.41	0.34	0.69	1.51	0.71	N/A	0.51	1.41
	Yellow River Basin	2.18	1.95	0.45	0.58	N/A	0.44	0.39	0.82	1.38	0.47	N/A	0.39	1.21
	Songhua - Liaohe River Basin	3.42	2.42	0.33	0.35	0.26	0.32	0.85	0.67	1.26	0.38	0.41	0.22	0.83
Total CSF ($t\ C\ km^{-2}\ yr^{-1}$)		5.80	5.31	0.87	0.62	0.88	1.14	1.73	1.25	1.72	1.07	3.75	0.89	2.53
Total CS ($Tg\ C\ yr^{-1}$)		4.42	6.98	0.69	0.04	0.02	0.34	0.05	0.22	3.12	1.49	0.07	0.23	17.69

Here, N/A indicates no CSF data for this type of rock in the region.

CSF produced by the same lithologies varied significantly from region to region. Thus, other influencing factors had a non-negligible influence on the weathering CSF of rocks.

3.1.2. Spatial distribution of the CSF and its influencing factors

Based on the GEM-CO_2 model, the weathering CSF of rocks in China was estimated from 2000 to 2014 (Fig. 1A). This did not include the unutilized areas in the northwest region and the Qinghai-Tibet region. The spatial distributions of the average annual CSF in the remaining areas were significantly different. Overall, the CSF was higher in most areas of the south and in southwestern Tibet. Particularly, areas with high CSF were distributed at the junction of Hunan, Guangxi, and Guangdong Provinces and the south of Shigatse. A CSF of less than 1 t C km^{-2} yr^{-1} accounted for approximately 47% of the Chinese terrestrial areas, whereas amounts that less than 5 t C km^{-2} a^{-1} accounted for approximately 82%.

As shown in Fig. 1B, the spatial distribution of China's annual average FVC was divided by the Hu Huanyong Line. It was characterized as low in the northwest and high in the southeast. The high-value areas were located in the northeastern region and the middle and upper reaches of the Yangtze River. Moreover, the low-value areas were located in the Xinjiang Basin. From 2000 to 2014, the average annual FVC was 0.52, with 42% of the FVC area less than 0.5 and 39% of the FVC area greater than 0.7.

Climate observations showed that the average annual temperature in China from 2000 to 2014 was in the range of −5.74 °C to 23.77 °C. Furthermore, China's temperature had evident regional characteristics in the spatial distribution. Regions below 0 °C were distributed in the Qinghai–Tibet Plateau, northeastern Inner Mongolia, and northeastern Heilongjiang. Regions above 20 °C were distributed in Hainan, Southern China, and southern Yunnan. The annual average precipitation was between 20 and 2922 mm. The characteristics of precipitation increased from the northwest to southeast. The northwest region was a low-

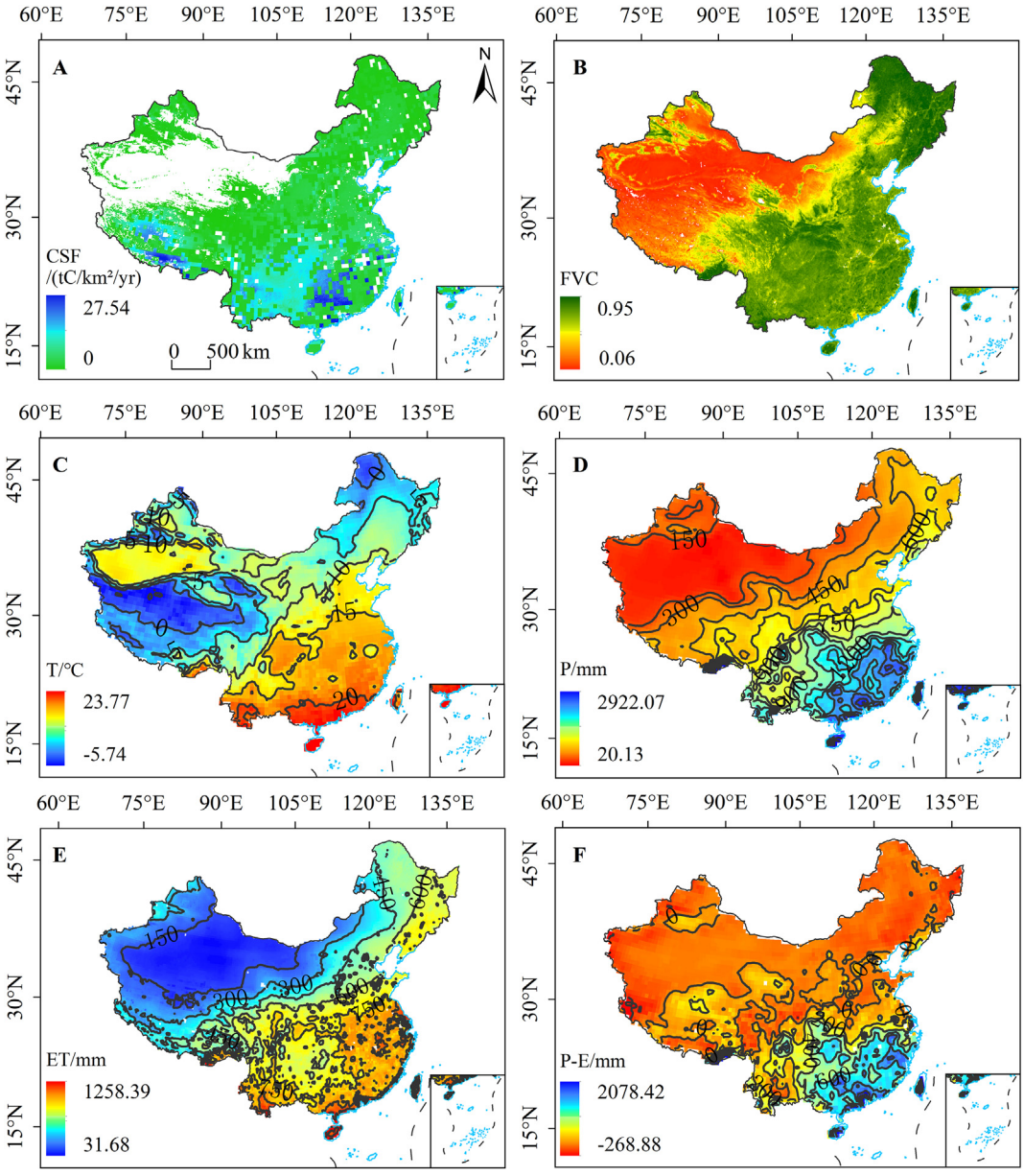

Fig. 1. Spatial distribution of the CSF and its influencing factors in China. CSF: Carbon Sink Flux; FVC: Fractional Vegetation Cover; T: Temperature; P: Precipitation; ET: Evapotranspiration; P-E: Water Budget.

value area of precipitation, whereas Hainan, Taiwan, and southern Tibet were the high-value areas of precipitation. The monsoon climate, rain belt movement, and climate change were the main atmospheric factors that led to the uneven spatial distribution of precipitation in China (Lü et al., 2018). The annual average evapotranspiration was between 31 and 1258 mm. This value decreased from the southeast coast to the northwest inland. The Continental Basin was the area of minimum evapotranspiration, whereas the Hainan, Taiwan, southern Yunnan, and southeastern coastal areas were areas with the maximum evapotranspiration. Precipitation is closely related to evapotranspiration, and it affects evapotranspiration by affecting the surface soil water content. A comparison of the spatial distribution of precipitation and evapotranspiration determined that the spatial distribution of the annual average water budget was more in the southeast and less in the northwest (Fig. 1C–F).

During the study period, the spatial distribution showed that the CSF was greater in the south and less in the north. FVC, temperature, precipitation, evapotranspiration, and water budget were all low in the southeast, but high in the northwest. The abovementioned results indicated that the spatial distribution of the magnitude of the CS had a feedback effect on the spatial distribution of factors, such as climate change and ecological restoration. The areas with mid-high values of FVC, temperature, precipitation, evapotranspiration, and water budget were also areas with mid-high values of the CSF distribution. In addition, areas with high-value precipitation and water budget were areas with the maximum CSF. However, Tibet, an area with low-value FVC and temperature also had a mid-high CSF given the distribution of carbonate rocks and mixed sedimentary rocks in the area. Moreover, the response sensitivity of the CSF for different influencing factors varied under diverse environments.

3.2. Spatiotemporal evolution of the CSF and its influencing factors

In terms of time evolution (Fig. 2), China's annual average CSF was in the range of 2.13–2.89 t C km^{-2} yr^{-1} during the study period, with minimal interannual variation. It reached its maximum in 2002 and reached its minimum in 2011, generally decreasing at a rate of 5.4 kg C km^{-2} yr^{-1}. The results showed that the annual average weathering CS slightly fluctuated in China and showed a slight decreasing trend.

Overall, the vegetation cover in China displayed a slight increasing trend, and the growth rate was approximately 7.8×10^{-3} yr^{-1}. Moreover, the increment was 0.056, and the increase was 12%. The maximum year for the average FVC was 2009, and the minimum year for the average FVC was 2004. The change in vegetation cover was primarily due to the implementation of numerous world-class key ecological restoration projects in China in addition to the implementation of the first round of the Grain-for-Green Project, which began in 1999. This resulted in an overall improvement in vegetation cover during the study period. However, China's average annual FVC showed a slight slowing down from 2010 to 2014. To adhere to the policy of a red line of 1.8 billion Mu (1.2 million km^2) farmland area, the project was suspended in 2007. The second phase of the project was restarted in 2014. There were significant achievements in China's ecological construction projects given the implementation of numerous major ecological protection and restoration projects during the study period.

The annual average temperature in China showed slow cooling after warming up. It reached a maximum value (9.1 °C) in 2007. The rate of warming during the study period was 0.01 °C yr^{-1}. The annual average precipitation showed a weakening trend prior to 2004 and reached a minimum (486 mm) in 2004. After this, it increased in volatility. Overall, it continued to rise at a rate of 3.4 mm yr^{-1}. The annual average evapotranspiration displayed a fluctuating upward trend within 15 years, and its growth rate reached 3.76 mm yr^{-1}. From 2000 to 2004, the annual average water budget decreased slowly and became an upward trend after 2004. The overall fluctuation was large, and water budget dropped slowly at a rate of −0.211 mm yr^{-1}.

The study period was relatively short for the observation of climate change, which may have resulted in the occurrence of years with outliers in the climate change factors. In general, the CSF and water budget displayed decreasing trends from 2000 to 2014, and the years in which they had peaks and valleys were 2000 and 2011. The total trends of FVC, temperature, precipitation, and evapotranspiration were all rising, in which the fluctuations in precipitation and water budget were significant. The correlation coefficient between the CSF and water budget was the highest, reaching 0.82, and the correlation coefficient between the CSF and precipitation was 0.65. Both coefficients showed positive correlations with the CSF. Temperature, evapotranspiration, and FVC were less correlated with the CSF, and their correlation coefficients were 0.25, 0.1, and 0.1, respectively. On this basis, the weathering CS of rocks displayed a sensitive response on climate change, especially for precipitation and water budget.

By further examining the evolution trend of the CSF and its influencing factors, the spatial distribution of the CSF evolution possessed

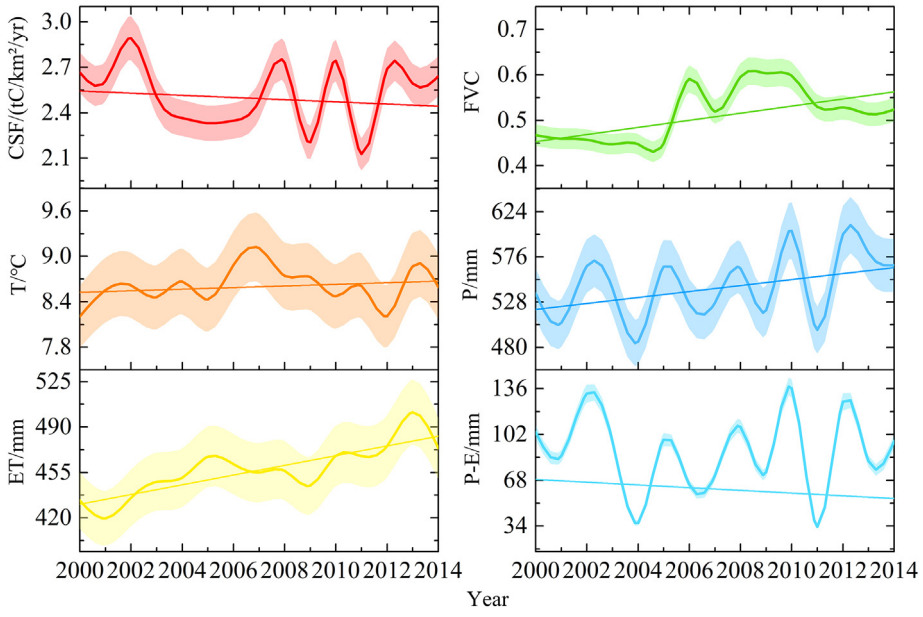

Fig. 2. Temporal evolution, fitting curve, and 5% error interval of the CSF and its influencing factors.

evident regional characteristics, and 57% of the CSF area showed an increasing trend. The largest increase in the CSF was located in the border area between Sichuan, Chongqing, and Guizhou. The areas with the largest reductions were Hunan, Yunnan, and southwestern Tibet (Fig. 3A).

As seen in Fig. 3B, the change areas of FVC were based on the low and high vegetation cover areas. Moreover, the stable areas were dominated by the middle cover area. The area ratio of FVC increasing was 86%. The Yangtze River Basin, the Pearl River Basin, the Southwest Basin, and the Yellow River Basin were areas where FVC obviously improved. FVC decreased significantly in northeast Inner Mongolia and northwest Xinjiang. In addition, accelerated urbanization and climate change has led to the deterioration of the ecological environment, thereby resulting in the sporadic reduction of regional FVC. In general, with the continuous increase in the national ecological and environmental protection efforts, the ecological environment in China has improved comprehensively, but the acceleration of urbanization will lead to a slight deterioration of the ecological environment in some areas (Fig. 3C–F).

During the study period, the area ratio of the temperature increase was 63%. The regions with significantly elevated temperatures were located in the Qinghai-Tibet Plateau and Yunnan. Also, the Songhua-Liaohe River Basin and the Haihe River Basin showed a significant decreasing trend. The areas that displayed an upward trend in precipitation accounted for 82% of the total area, which was much larger than its reduced area. The areas that displayed a significant increase in precipitation were located along the borders of Jiangsu, Zhejiang, Guangxi, and Guangdong. In addition, the areas that displayed reduced precipitation were located in Yunnan. The area of evapotranspiration that showed an increasing trend accounts for 81%, with obvious increases reported in the northeast region and the Pearl River Basin. The area that displayed a decreasing trend in water budget was larger than the area with a decreasing trend in precipitation. In addition, the decreasing regional ratio of water budget was 51%, which was 2.8 times the area of precipitation reduction.

By comparing the spatial distribution of the CSF and its influencing factors, the reduced area in the southern part of the CSF was a region where water budget was shown to be significantly reduced, and it was

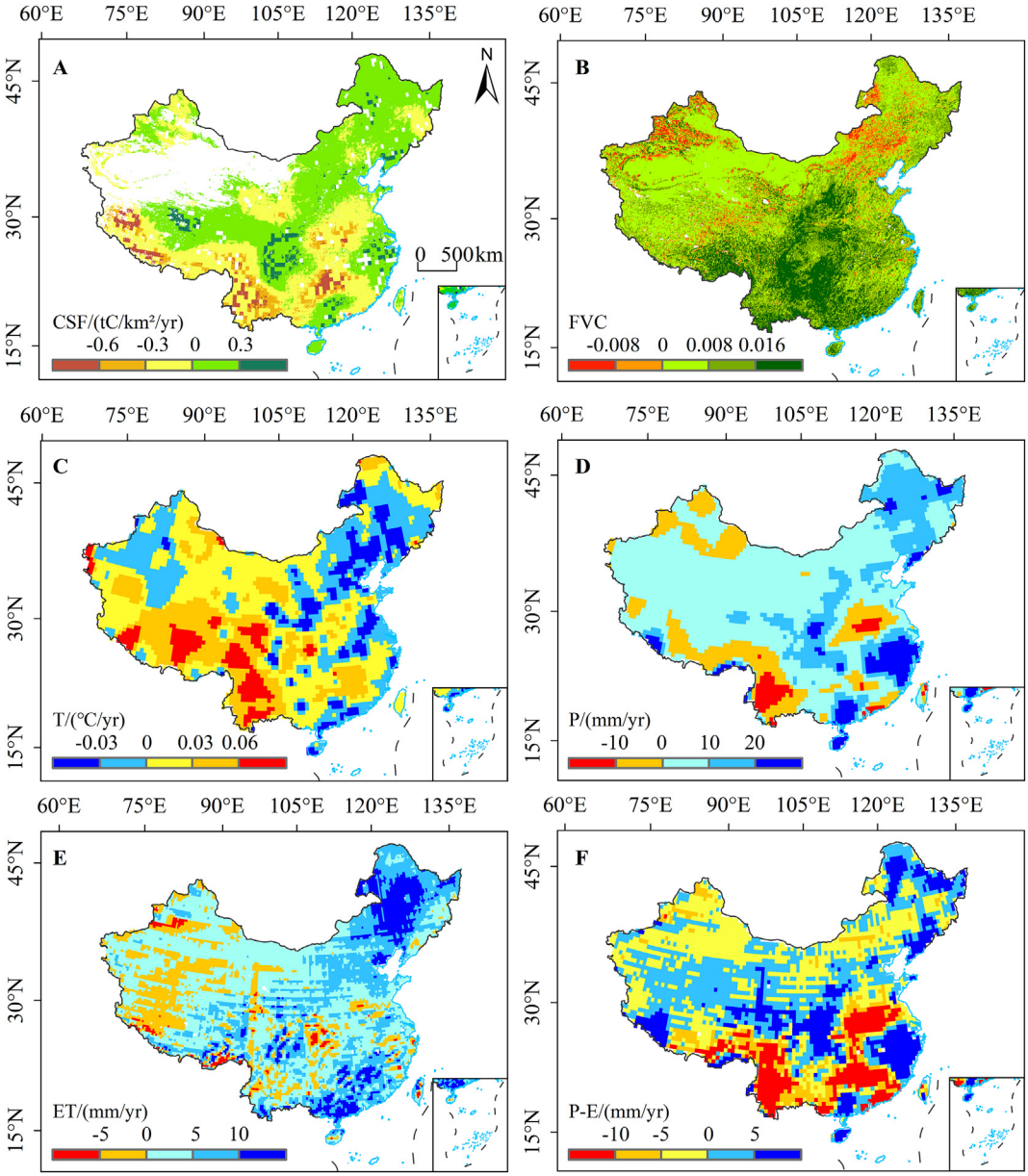

Fig. 3. Spatial evolution trend of the CSF and its influencing factors.

also an area where the temperature was shown to be rising and the precipitation decreasing. The areas of decreased CSF in the north were locations with reduction areas of water budget and FVC. The area with a large increase in the CSF was the area where water budget, precipitation, and evapotranspiration were shown to be increasing. The spatial distribution of the CSF evolution trend was affected by the spatial distribution of the evolution of its influencing factors. Therefore, the weathering CS of rocks can rapidly respond to climate change and ecological restoration. However, different factors have various effects on the weathering CS of rocks, and the response of the weathering CS to each factor is different in different areas. Therefore, the influence of the factors of the CSF in different areas needs to be assessed quantitatively to accurately analyze the driving factors of the weathering CS of rocks.

3.3. Impact of climate change and ecological restoration on the CS

The effects of temperature, precipitation, evapotranspiration, water budget, and FVC on the CSF of rock weathering were analyzed, and the relative contribution rates of each factor to CSF were obtained. Fig. 4 shows that the response of the CSF to various influencing factors varied significantly in the different basins. However, in addition to the Continental Basin, precipitation and water budget were the decisive factors that affected the CSF, and they had a proportional contribution. The relative contribution rate of temperature in the Southwest Basin reached 28%, and its values in the Haihe River Basin and the Songhua-Liaohe River Basin, where the temperature drops significantly, was 19% and 14%, respectively. Therefore, the CSF responds to the temperature changes evidently in the low-temperature and temperature-drop areas. The relative contribution rate of evapotranspiration was higher in the Haihe River Basin and the Yangtze River Basin than in the other basins, and its contribution rate was less than 6% in the other basins. In the Continental Basin, where FVC was low overall and precipitation was poor, the relative contribution rate of FVC was the largest, reaching 74%. The Continental Basin had large areas of CSF with null values, and these areas were also the low-value areas for precipitation, evapotranspiration, water budget, and FVC. Therefore, the relative contribution rate of other factors, except FVC, was low in these areas. At the national scale, water budget was the most important driving factor of the CSF, with a relative contribution rate of 57%. In addition, the response of the CSF to precipitation change was also evident, reaching 35%. The CSF was also affected by other factors. The relative contribution of temperature was 6%. Evapotranspiration and FVC accounted for only 1%. Therefore, the CSF is not primarily controlled by the abovementioned three factors.

According to the analysis of the relative contribution of the factors to the CSF at different scales, it appears that precipitation and water budget were the decisive factors that affected the weathering CS of rocks. The relative contribution rates of temperature and evapotranspiration were less than the abovementioned decisive factors, but they also produced an important impact on the CSF. The relative contribution rate of temperature was higher in the low-temperature and temperature-decreasing areas than in other areas. The relative contribution rate of evapotranspiration in the different basins did not show a certain regularity. Therefore, the water environment characteristics in a region must be considered in combination with the precipitation conditions to accurately determine its influence on the CSF. Furthermore, an improved water environment signifies an increasingly active weathering process. In comparison with the abovementioned factors, the relative contribution rate of FVC to the CSF was primarily weak. However, in the low-value areas of FVC, FVC had important influences on the CSF. By quantifying the relative contribution rates of the various influencing factors, it was demonstrated that CSF could respond rapidly to climate change and ecological restoration, thereby affecting the global carbon cycle and the carbon budget.

3.4. Evolution comparison and response of the weathering CSF in different lithologies

3.4.1. Evolution comparison of the CSF in different lithologies

By analyzing the different time evolutions of the CSF in the 12 types of rocks in China during the study period (Fig. 5), the CSFs of carbonate

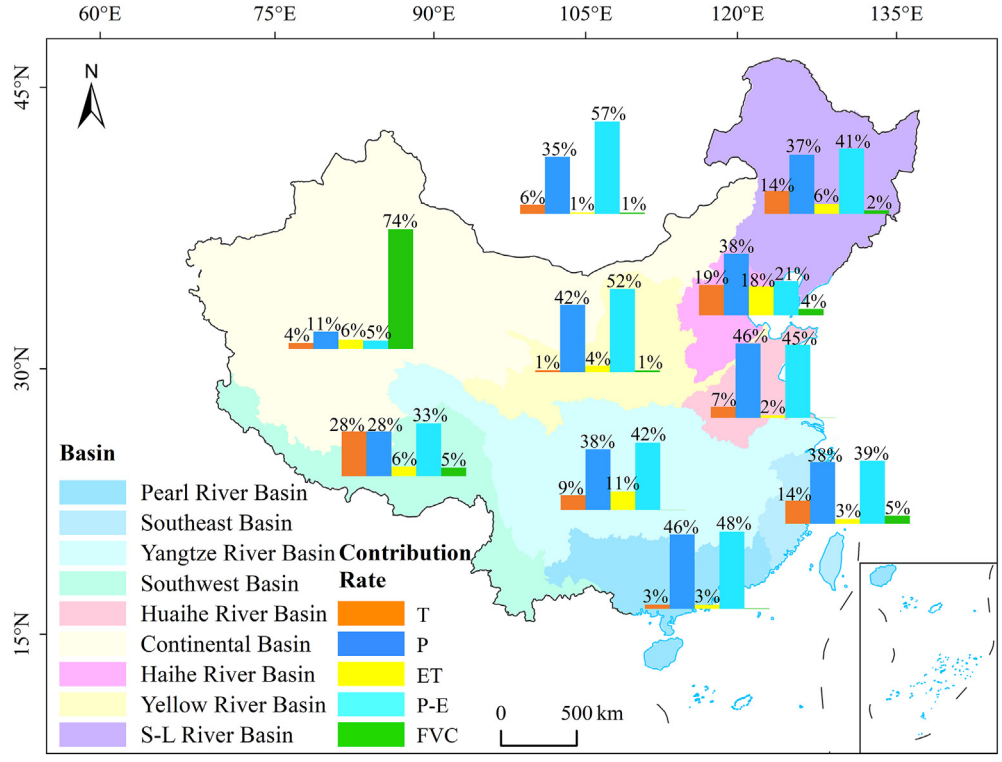

Fig. 4. Relative contribution rates of the impact factors to the CSF in the different basins.

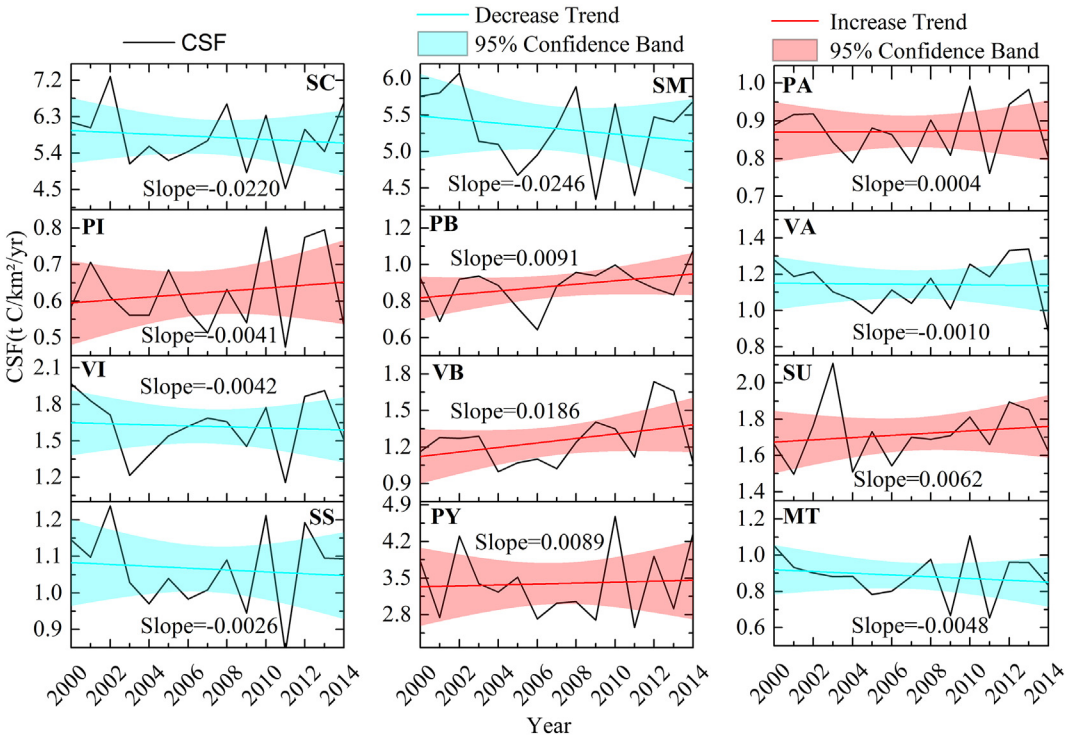

Fig. 5. Temporal evolution characteristics of the CSF with different lithologies. SC: Carbonate Rocks; SM: Mixed Sedimentary Rocks; PA: Acid Plutonic Rocks; PI: Intermediate Plutonic Rocks; PB: Basic Plutonic Rocks; VA: Acid Volcanic Rocks; VI: Intermediate Volcanic Rocks; VB: Basic Volcanic Rocks; SU: Unconsolidated Sediments; SS: Siliciclastic Sediments Rocks; PY: Pyroclastic; MT: Metamorphic Rocks.

rocks, mixed sedimentary rocks, basic volcanic rocks, intermediate volcanic rocks, siliciclastic sediments rocks, and metamorphic rocks all showed decreasing trends. In contrast, the CSF of the remaining rocks showed an increasing trend. Mixed sedimentary and carbonate rocks had more evident reduction trends in the CSF than in other rocks, and their decreasing rates were −0.0246 and −0.022 t C km^{-2} yr^{-1}, respectively. The most significant increase in the CSF was in acid volcanic rocks, with an increase rate of 0.0186 t C km^{-2} yr^{-1}. The annual average CSF of carbonate rocks, mixed sedimentary rocks, unconsolidated sediments, and siliciclastic sediments rocks reached their peaks in 2002. Moreover, the CSF of carbonate rocks, basic plutonic rocks, intermediate plutonic rocks, intermediate volcanic rocks, siliciclastic sediments rocks, pyroclastic, and metamorphic rocks all reached their valleys in 2011. In addition, numerous similarities were observed in the evolutionary trends of carbonate rocks and mixed sedimentary rocks, and the CSF evolution trends of basic plutonic rocks and intermediate plutonic rocks also showed some similarities. Different rocks have various lithologies, but the tendency to change the CSF under the combined effects of climate change, ecological restoration, and other factors remains consistent. Therefore, the weathering CS of rocks is controlled by their lithology, but they also have a sensitive response on external environmental changes.

3.4.2. Impacts of climate change and ecological restoration on the CS under different lithologies

In Fig. 6, the responses of the different lithological CSFs to each impact factor were different. However, in addition to basic volcanic rocks and intermediate volcanic rocks, water budget and precipitation had relatively high contribution rates to the CSF of other lithologies. The CSFs of carbonate rocks, mixed sedimentary rocks, intermediate plutonic rocks, acidic volcanic rocks, and unconsolidated sediments showed some feedback on temperature and evapotranspiration. Furthermore, the influence of FVC on the abovementioned five types of lithological CSFs was weak. For basic plutonic rocks, siliciclastic sediments rocks, pyroclastic, and metamorphic rocks, except for the significant impacts from water budget and precipitation, temperature also accounted for a certain proportion of the relative contribution rate. However, the relative contribution rates of evapotranspiration and FVC were low. The relative contribution rate of water budget to acid plutonic rocks was the most significant, followed by precipitation, FVC, temperature, and evapotranspiration. The contribution rates of FVC, temperature, and evapotranspiration were low. The effect of temperature on the CSF was significantly higher in basic volcanic rocks and intermediate plutonic rocks than in other types of rocks, and the effect of precipitation on the abovementioned two types of rocks was less than the influence of temperature.

Therefore, the different types of rocks with scattered distributions had obvious responses to water budget and precipitation changes. Temperature and evapotranspiration also accounted for a certain proportion of the relative contribution rate. The influence of FVC on the CSF was weak. These results were different from those obtained using the basin division, primarily because the relative contribution rate of FVC in the Continental Basin was abnormally high. Therefore, the relative contribution rate of each impact factor to the CSF was different under various division modes.

4. Discussion

4.1. Comparison with other related studies

The results obtained in this study were compared with the relevant research results from different scales to explain the accuracy and reliability of the calculation results further. Qiu used the same GEM-CO_2 model as this study to investigate the weathering CS of rocks in China (Qiu et al., 2004). This author calculated the CS in China as 14.1 Tg C yr^{-1} and the CSF as 1.64 t C km^{-2} yr^{-1}. In contrast, the results obtained in this study were 17.69 Tg C yr^{-1} and 2.53 t C km^{-2} yr^{-1}, correspondingly. Considering Chinese rock species were divided into 9 species in Qiu's research, whereas 12 rock species were used in this study. The differences in the research period, source, and accuracy of data could also lead to differences in results. Liu (Liu and Wolfgang, 2012) and Li (Li et al., 2019a) calculated the carbonate CS in China using the

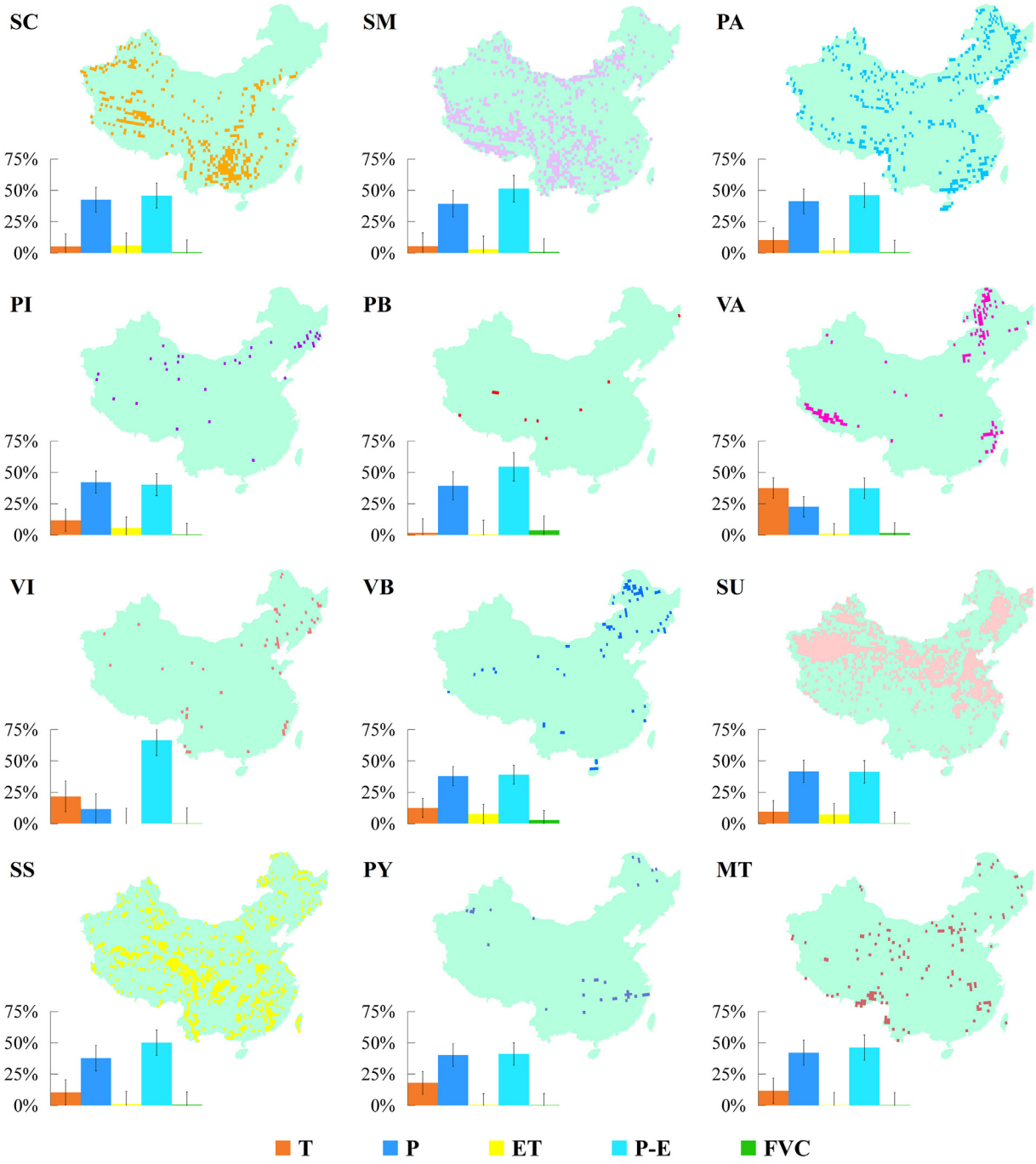

Fig. 6. Distribution of different lithologies and the relative contribution rate of each impact factor to the CSF of various lithologies in terrestrial China.

hydrochem-discharge method and the maximum potential dissolution method. The carbonate CSF obtained using the two methods were 10.4 and 5.02 t C km^{-2} yr^{-1}, and the result of this study was 6.41 t C km^{-2} yr^{-1}, which is between the above two results. This indicates that different models, input data, and research focus can underestimate or overestimate the CSF. Some differences were also observed between the results of this study and those of other studies based on different basins. This was likely due to differences in the regions that were studied, the methods of estimation, and other factors. Currently, most studies on the weathering CS of rocks in China have focused on the weathering process of carbonate rocks and silicate rocks, and studies on the weathering CS of other types of rocks have been relatively scarce. Therefore, only the current magnitudes of CSs and CSFs of carbonate rocks and silicate rocks were compared, as shown in Table 2. The results of this study differed somewhat from those of other studies, but these differences were due to a combination of different factors. A comparison of CSs and CSFs in different basins and lithologies showed that the GEM-CO_2 model had a high reliability in China, and the results of this study have a high degree of credibility and feasibility.

In studying the effects of climate change and other factors on the weathering CS of rocks, Gislason concluded that in the eight watersheds of Iceland, chemical weathering increased by 4%–14% with an increase in the air temperature of 1 °C (Gislason et al., 2009). Liu estimated that global warming may lead to a 21% increase in the global carbonate CS by 2100 (i.e., approximately 0.18 Pg C yr^{-1}) (Liu and Wolfgang, 2012). Beaulieu suggested that a high sensitivity of CO_2 consumed by terrestrial weathering to climate and land-use changes (Beaulieu et al., 2012). Zeng confirmed the importance of climate influence in the

Table 2
Comparison of rock CSs at different scales.

Areas	CS ($Tg\ C\ yr^{-1}$)	CS in this study ($Tg\ C\ yr^{-1}$)	CSF ($t\ C\ km^{-2}\ yr^{-1}$)	CSF in this study ($t\ C\ km^{-2}\ yr^{-1}$)
Yangtze River Basin (Amiotte et al., 2003)	4.82[c]	1.83[c]	4.95[c]	6.62[c]
	0.48[s]	0.92[s]	0.61[s]	1.41[s]
Yangtze River Basin (Gaillardet et al., 1999)	1.28[s]		0.71[s]	
Yellow River Basin (Fan et al., 2014)	0.31[s]	0.11[s]	0.42[s]	0.47[s]
Yellow River Basin (Li and Zhang, 2003)	1.06[c]	0.86[c]	5.74[c]	2.18[c]
Pearl River Basin (Cao et al., 2011)	1.85[c]	1.28[c]	11.68[c]	8.79[c]
Guizhou (Zeng et al., 2016)	1.56[c]	1.12[c]	10.3[c]	7.12[c]
China (Qiu et al., 2004)	14.1[a]	17.69[a]	1.64[a]	2.53[a]
	7.45[c]	4.42[c]	7.49[c]	5.8[c]
China (Liu and Wolfgang, 2012)	36[c]		10.4[c]	
China (Liet al., 2019)	11.37[c]		5.02[c]	

Green columns: other studies; blue columns: this study.
a: all kinds of rocks; c: carbonate rocks; s: silicate rocks.

carbonate CS by analyzing the correlation between changes in the carbonate CS and climate change in Southwest China from 1970 to 2013. This researcher also reported that runoff depth and precipitation were the primary driving factors for CS changes in carbonate rocks. Temperature and the equilibrium concentration of carbonate rocks also affect the strength of the CS of karstification, but the carbonate CS in Southwest China was not main controlled by these two factors (Zeng et al., 2016b). Li considered that the mean runoff modulus (q) was a key factor that affected the carbonate CS, which was primarily influenced by factors such as climate, topography, and vegetation (Li et al., 2019b).

4.2. Response mechanism and significance of the weathering CS in rocks

By combining the temporal change and spatial distribution of the evolution trend of the CSF and its influencing factors, it was shown that a decreasing water budget had a negative impact on the weathering CSF in rocks, and an increase in temperature also led to a decrease in the CSF. In the distribution of the spatial evolution, reductions in precipitation and evapotranspiration decreased the CSF. In the evolution of time, precipitation displayed an increasing trend during the study period, but the CSF was slightly reduced. The reason is that evapotranspiration increased, and the combined effect of precipitation and evapotranspiration led to a decrease in water budget, so that the CSF reduced. The restoration of FVC had a positive impact on the CSF. But FVC showed a low relative contribution rate to the CSF, and the influences of the other factors counteracted its effect.

The conclusion is drawn from the factors mentioned above, that water availability is a key to chemical rock weathering, and high water availability promotes chemical rock weathering. The relative contribution of water budget to the CSF was high in this study because positive water budget increased water availability. Water availability is also affected by other factors, precipitation and evapotranspiration affect water availability by affecting water budget. High temperature could generally reduce water availability by causing quicker evaporation both from soil and vegetation. FVC could be more important in arid areas because of the water retention functions of vegetation increase water availability. Therefore, water availability could be considered as an important factor for the CSF. Therefore, various factors should be comprehensively considered together to determine how the CSF is affected.

The difference between the carbon source (carbon emission) and the CS is termed a missing CS (Schimel, 1995). Houghton estimated that the anthropogenic carbon emission to the atmosphere (7.1 Pg C yr^{-1}) was more than the sum of carbon accumulated in the atmosphere (3.3 ± 0.2 Pg C yr^{-1}) and absorbed by the ocean (2.0 ± 0.8 Pg C yr^{-1}). Therefore, the missing CS was approximately 1.8 Pg C yr^{-1} (Houghton et al., 1998). Melnikov and O'Neill found that the large terrestrial missing CS was 2.8 Pg C yr^{-1} (Melnikov and O'Neill, 2006). The weathering CS (17.69 Tg C yr^{-1}) in terrestrial rocks in China, which was calculated in this study,

accounted for 1% and 0.6% of the above missing CS, respectively. According to Xu, the magnitude of the carbon emission was 1.01 Pg C yr^{-1} (2000–2004) in China (Xu et al., 2006). Therefore, the weathering CS in terrestrial rocks was equivalent to 1.8% of carbon emission.

To explore the mechanism and location of the terrestrial missing CS, many researchers have focused on the roles of the soil CS (Liu et al., 2020) and the vegetation CS. According to this study, the weathering CS of rocks was equivalent to 7%–9% of the total terrestrial ecosystem CS (0.19–0.26 Pg C yr^{-1}) (Piao et al., 2009) and equivalent to 25%–43% of the soil CS (41–71 Tg C yr^{-1}) (Fang et al., 2007) in China. In addition, China accounted for approximately 6.44% of the world's land area, and its CS was equivalent to 6.8% of the global CS of rocks (0.26 Gt C yr^{-1}) (Suchet and Probst, 1995). Whether in China or in the world, the weathering CS of rocks is a significant portion of terrestrial ecosystem CS. It also occupies a certain proportion of the missing CS and carbon emission. Thus, it is very significant to explore the magnitude, distribution, evolution, and influencing factors of the weathering CS of rocks when researching on the carbon cycle and its global changes.

4.3. Limitations of the study and future scope

In this study, some problems emerged in data selection and data matching of different precisions. The sources of input data are different, the accuracy of result estimation is therefore different. Hence, the reliability of the selected data must be improved. Simultaneously, the model itself may have some limitations, and its empirical coefficient *a* must be verified by numerous actual experimental results and repeated verification in the future to improve its accuracy and applicability to different regions. Thus, improving the estimation ability of the model is the emphasis and difficulty of present and future research. There is no unique unchallenged metric of relative importance in case of correlated regressors (Ulrike, 2006). Therefore, the LMG model that was used to estimate relative importance also had some limitations, and this may have led to some deviations in the calculation of the relative importance results. The development of a more procedure to evaluate the relative importance is the goal of future work.

The calculation of water budget should take into account the water transfer due to runoff and other factors. This study referred to the calculation of the weathering carbon sink of rocks by other researchers, so this factor was not considered in water budget. But runoff is not only important to water budget, but also affects the weathering carbon sink of rocks (Raymond, 2003; Raymond et al., 2008). Other environmental factors, such as the PH of precipitation (Oliva et al., 2003), respiration of plants and soil microorganisms (Davidson and Janssens, 2006; Wan et al., 2007), exposed rock area (Probst et al., 1994), and physical erosion processes (West et al., 2005; Gaillardet et al., 1999) will also impact the rock CS. In this study, only several factors were considered, and the relative contribution rate of each factor will change accordingly when other relevant factors are added. Therefore, the results obtained in this study are not very comprehensive. The influencing factors must be fully considered in the future research. In addition, interactions between the influencing factors on the weathering CS of rocks must be further explored.

5. Summary

The weathering CS of terrestrial rocks in China from 2000 to 2014 was estimated using the GEM-CO_2 model. The results showed that:

(1) For the time period of 2000–2014, the CS of terrestrial rocks in China was 17.69 Tg C yr^{-1}, and the CSF was 2.53 t C km^{-2} yr^{-1}. Mixed sedimentary rocks had the highest CS (6.89 Tg C yr^{-1}) of the 12 types of rocks, and carbonate rocks had the highest CSF (5.8 t C km^{-2} yr^{-1}). In the nine major river basins, the Pearl River Basin had the highest CSF (5.96 t C km^{-2} yr^{-1}), whereas the CSF in the Songhua-Liaohe River Basin was the lowest (0.83 t C km^{-2} yr^{-1}), and the difference between the two was approximately seven times.

(2) The weathering CS of rocks in China was high in the south and low in the north according to the spatial distribution, and the high-value areas were distributed at the junction of Hunan, Guangxi, and Guangdong and the south of Shigatse. FVC, temperature, precipitation, evapotranspiration, and water budget were all high in the southeast but low in the northwest. The spatial distribution of the magnitude of the CS had a significant feedback effect on the spatial distribution of climate change and ecological restoration.

(3) In terms of time evolution, the CSF during the study period decreased slowly at a rate of 5.4 kg C km^{-2} yr^{-1} in China, and water budget also displayed a downward trend. However, the general trends of FVC, temperature, precipitation, and evapotranspiration all increased. Furthermore, the correlation coefficient between water budget and the CSF was the highest (reaching 0.82), and the correlation coefficient between precipitation and the CSF was 0.65. For the spatial evolutionary trend, the reduced area in the southern part of the CSF was a region where the water budget was significantly reduced. It was also an area where the temperature increased and the precipitation decreased. The areas of decreasing CSF in the north had reduced water budget and FVC.

(4) At the national scale, the relative contribution rates of water budget and precipitation were 57% and 35%, respectively, followed by temperature, with a contribution rate of 6%. The contribution rates of evapotranspiration and FVC were only 1%. The relative contribution rate of temperature was higher in the low-temperature and temperature-decreasing area than in other areas. The relative contribution rate of FVC to the CSF was primarily weak. However, in the Continental Basin, where FVC was low overall, the relative contribution rate of FVC was the largest, reaching 74%. Additionally, the above factors influenced rock weathering by jointly affecting water availability. It was verified that the CSF could respond rapidly to climate change and ecological restoration by quantifying the relative contribution rates of the various influencing factors, thereby affecting the global carbon cycle and the carbon budget.

(5) During the study period, the CSF of six types of rocks displayed decreasing trends, whereas that of the remaining rocks displayed increasing trends. The two types of rocks with more evident reduction trends in the CSF than other rocks were mixed sedimentary and carbonate rocks, and their reduction rates were −0.0246 and −0.022 t C km^{-2} a^{-1}, respectively. The most significant increase in the CSF was from acidic volcanic rocks, with a slope of 0.0186 t C km^{-2} a^{-1}. With the exception of the evident responses from basic volcanic rocks and intermediate volcanic rocks to temperature changes, the relative contribution rates of water budget and precipitation to different lithologic CSFs were dominant. The contribution rates of temperature, evapotranspiration, and FVC were all low.

CRediT authorship contribution statement

Suhua Gong: Conceptualization, Methodology, Software, Writing - original draft. **Shijie Wang:** Supervision, Project administration. **Xiaoyong Bai:** Conceptualization, Resources, Supervision, Project administration. **Guangjie Luo:** Resources, Writing - review & editing. **Luhua Wu:** Writing - review & editing, Data curation. **Fei Chen:** Writing - review & editing, Investigation. **Qinghuan Qian:** Writing - review & editing. **Jianyong Xiao:** Writing - review & editing. **Cheng Zeng:** Writing - review & editing.

Declaration of competing interest

No conflict of interest exists in the submission of this manuscript, and all authors approved the manuscript and this submission. I declare on behalf of my co-authors that the manuscript described is an original work that has not been published previously and not under consideration for publication elsewhere, in whole or in part.

Acknowledgments

This research work was supported jointly by National Key Research Program of China (No. 2016YFC0502300 & 2016YFC0502102), Western Light Talent Program (Category A) (No. 2018–99), United Fund of Karst Science Research Center (No. U1612441), Science and Technology Plan of Guizhou Province of China (2017–2966), Chinese Academy of Science and Technology Services Network Program (No. KFJ–STS–ZDTP–036) and International Cooperation Agency International Partnership Program (No. 132852KYSB20170029, No. 2014–3), International Cooperation Research Projects of the National Natural Science Fund Committee (No. 41571130074 & 41571130042).

References

Amiotte, S., Probst, J.L., 1993. Flux de CO_2 consommé par altération chimique continentale: Influences du drainage et de la lithologie. C R Acad Sci Paris 317, 615–622.

Amiotte, S., Probst, J.L., Ludwig, W., 2003. Worldwide distribution of continental rock lithology: implications for the atmospheric/soil CO_2 uptake by continental weathering and alkalinity river transport to the oceans. Glob. Biogeochem. Cycles 17 (2). https://doi.org/10.1029/2002gb001891.

Beaulieu, E., Goddéris, Y., Donnadieu, Y., Labat, D., Roelandt, C., 2012. High sensitivity of the continental-weathering carbon dioxide sink to future climate change. Nat. Clim. Chang. 2 (5), 346–349. https://doi.org/10.1038/nclimate1419.

Burton-Chellew, M.N., May, R.M., West, S.A., 2013. Combined inequality in wealth and risk leads to disaster in the climate change game. Clim. Chang. 120 (4), 815–830. https://doi.org/10.1007/s10584-013-0856-7.

Cao, J., Yang, H., Kang, Z., 2011. Preliminary regional estimation of carbon sink flux by carbonate rock corrosion: a case study of the Pearl River Basin. Chin. Sci. Bull. 56 (35), 3766–3773. https://doi.org/10.1007/s11434-011-4377-3.

Davidson, E.A., Janssens, I.A., 2006. Temperature sensitivity of soil carbon decomposition and feedbacks to climate change. Nature 440 (7081), 165–173. https://doi.org/10.1038/nature04514.

Fan, B.L., Zhao, Z.Q., Tao, F.X., Liu, B.J., Tao, Z.H., Gao, S., Zhang, L.H., 2014. Characteristics of carbonate, evaporite and silicate weathering in Huanghe River basin: a comparison among the upstream, midstream and downstream. J. Asian Earth Sci. 96, 17–26. https://doi.org/10.1016/j.jseaes.2014.09.005.

Fang, J.Y., Chen, A.P., Peng, C.H., Zhao, S.Q., Ci, L.J., 2001. Changes in forest biomass carbon storage in China between 1949 and 1998. Science 292 (5525), 2320–2322. https://doi.org/10.2307/3083885.

Fang, J., Guo, Z., Piao, S., Chen, A., 2007. Terrestrial vegetation carbon sinks in China, 1981–2000. Sci. China Ser. D Earth Sci. 50 (9), 1341–1350. https://doi.org/10.1007/s11430-007-0049-1.

Fang, J.Y., Guo, Z.D., Hu, H.F., Kato, T., Muraoka, H., Son, Y., 2014. Forest biomass carbon sinks in East Asia, with special reference to the relative contributions of forest expansion and forest growth. Glob. Chang. Biol. 20 (6), 2019–2030. https://doi.org/10.1111/gcb.12512.

Gaillardet, J., Dupré, B., Louvat, P., Allègre, C.J., 1999. Global silicate weathering and CO_2 consumption rates deduced from the chemistry of large rivers. Chem. Geol. 159 (1–4), 3–30. https://doi.org/10.1016/s0009-2541(99)00031-5.

Gaillardet, J., Calmels, D., Romero-Mujalli, G.Z., Hartmann, J., 2018. Global climate control on carbonate weathering intensity. Chem. Geol., 05–009 https://doi.org/10.1016/j.chemgeo05.009.

Gao, G., Xu, C.Y., 2015. Characteristics of water surplus and deficit change in 10 major river basins in China during 1961-2010. Acta Geol. Sin. 70 (3), 380–391. https://doi.org/10.11821/dlxb201503003.

Gislason, S.R., Oelkers, E.H., Eiriksdottir, E.S., 2009. Direct evidence of the feedback between climate and weathering. Earth Planet. Sci. Lett. 277 (1–2), 213–222. https://doi.org/10.1016/j.epsl.2008.10.018.

Gombert, P., 2002. Role of karstic dissolution in global carbon cycle. Glob. Planet. Chang. 33 (1–2), 177–184. https://doi.org/10.1016/s0921-8181(02)00069-3.

Houghton, R.A., Davidson, E.A., Woodwell, G.M., 1998. Missing sinks, feedbacks, and understanding the role of terrestrial ecosystems in the global carbon balance. Global Biogeochemical Cycles 12 (1), 25–34. https://doi.org/10.1029/97gb02729.

Kennedy, D., 2001. Breakthrough of the year. Science 294, 2443–2447. https://doi.org/10.1126/science.294.5551.2429.

Kheshgi, H.S., Jain, A.K., Wuebbles, D.J., 1996. Accounting for the missing carbon-sink with the CO_2-fertilization effect. Clim. Chang. 33 (1), 31–62. https://doi.org/10.1007/bf00140512.

Leighton, M.T., 2011. Climate Change and Migration: Rethinking Policies for Adaptation and Disaster Risk Reduction. Publication Series of United Nations University.

Li, J., Zhang, J., 2003. Chemical weathering processes and atmospheric CO_2 consumption in the yellow river drainage basin. Mar. Geol. Quat. Geol. 23, 43–49.

Li, H., Wang, S., Bai, X., Cao, Y., Wu, L., 2019a. Spatiotemporal evolution of carbon sequestration of limestone weathering in China. Science China Earth Sciences 62 (6), 974–991. https://doi.org/10.1007/s11430-018-9324-2.

Li, C., Wang, S., Bai, X., et al., 2019b. Estimation of carbonate rock weathering-related carbon sink in global major river basins. Acta Geograph. Sin. 74 (07), 1319–1332. https://doi.org/10.11821/dlxb201907004.

Liu, J., Han, G., 2020. Major ions and $d^{34}S_{SO4}$ in Jiulongjiang River water: Investigating the relationships between natural chemical weathering and human perturbations. Sci. Total Environ. 724, 138208. https://doi.org/10.1016/j.ecitotenv.2020.138208.

Liu, M., Han, G., Zhang, Q., 2020. Effects of agricultural abandonment on soil aggregation, soil organic carbon storage and stabilization: Results from observation in a small karst catchment, Southwest China. Agric. Ecosyst. Environ. 288, 106719. https://doi.org/10.1016/j.agee.2019.106719.

Liu, Z., Wolfgang, D., 2012. Comparison of carbon sequestration capacity between carbonate weathering and forests: the necessity to change traditional ideas and methods of study of carbon sinks. Carsologica Sinica 31, 345–348. https://doi.org/10.3969/j.issn.1001-4810.2012.04.001.

Liu, Z., Zhao, J., 2000. Contribution of carbonate rock weathering to the atmospheric CO_2 sink. Environ. Geol. 39 (9), 1053–1058. https://doi.org/10.1007/s002549900072.

Liu, Z., Dreybrodt, W., Wang, H., 2010. A new direction in effective accounting for the atmospheric CO_2 budget: considering the combined action of carbonate dissolution, the global water cycle and photosynthetic uptake of DIC by aquatic organisms. Earth Sci. Rev. 99 (3–4), 162–172. https://doi.org/10.1016/j.earscirev.2010.03.001.

Lü, L., Kong, F., Wang, P., 2018. Spatial difference analysis of evolution characteristics of the four seasons rainfall events in 1961~2016 of China. Science Technology and Engineering 18 (22), 1–14. https://doi.org/10.3969/j.issn.1671-1815.2018.22.001.

Martin, J.B., 2016. Carbonate minerals in the global carbon cycle. Chem. Geol. 449, 58–72.

Melnikov, N.B., O'Neill, B.C., 2006. Learning about the carbon cycle from global budget data. Geophys. Res. Lett. 33 (2). https://doi.org/10.1029/2005gl023935.

Meybeck, M., 1979. Concentrations des eauxfluviales en elements majeurs et apports en solution aux oceans. Rev Géol Dynam Géogr Phys. 21, 215–246.

Meybeck, M., 1987. Global chemical weathering of surficial rocks estimated from river dissolved loads. Am. J. Sci. 287 (5), 401–428. https://doi.org/10.2475/ajs.287.5.401.

Oliva, P., Viers, J., Dupré, B., 2003. Chemical weathering in granitic environments. Chem. Geol. 202 (3–4), 225–256. https://doi.org/10.1016/j.chemgeo.2002.08.001.

Piao, S., Fang, J., Ciais, P., Peylin, P., Huang, Y., Sitch, S., Wang, T., 2009. The carbon balance of terrestrial ecosystems in China. Nature 458 (7241), 1009–1013. https://doi.org/10.1038/nature07944.

Post, W.M., Chavez, F., Mulholland, P.J., Pastor, J., Peng, T.H., Prentice, K., Webb, T., 1992. Climatic feedbacks in the global carbon cycle. The Science of Global Change, 392–412 https://doi.org/10.1021/bk-1992-0483.ch021.

Probst, J.L., Amiotte, S.P., Tardy, Y., 1992. Global continental erosion and fluctuations of atmospheric CO_2 consumed during the last 100 years. In: Kharaka, Y.K., Maest, A. (Eds.), Proc 7th Int Symp. W R I. Park City, Utah, USA. Balkema, Rotterdam, pp. 483–486.

Probst, J.L., Mortatti, J., Tardy, Y., 1994. Carbon river fluxes and weathering CO_2 consumption in the Congo and Amazon river basins. Appl. Geochem. 9 (1), 1–13. https://doi.org/10.1016/0883-2927(94)90047-7.

Qin, X., Liu, P., Huang, Q., Zhang, L., 2013. Estimation of atmospheric/soil CO_2 consumption by rock weathering in the Pearl River Valley. Acta Geosci. Sin. 34, 455–462. https://doi.org/10.3975/cagsb.2013.04.08.

Qiu, D., Zhuang, D., Hu, Y., et al., 2004. Estimation of carbon sink capacity caused by rock weathering in China. Earth Science Journal of China University of Geosciences 29, 177–183. https://doi.org/10.3321/j.issn:1000-2383.2004.02.009.

Raymond, P.A., 2003. Increase in the export of alkalinity from North America's Largest River. Science 301 (5629), 88–91. https://doi.org/10.1126/science.1083788.

Raymond, P.A., Oh, N.H., Turner, R.E., Broussard, W., 2008. Anthropogenically enhanced fluxes of water and carbon from the Mississippi River. Nature 451 (7177), 449–452. https://doi.org/10.1038/nature06505.

Romero-Mujalli, G.J., Hartmann, B., 2018. Temperature and CO_2 dependency of global carbonate weathering fluxes - implications for future carbonate weathering research. Chem. Geol. https://doi.org/10.1016/j.chemgeo.

Schimel, D.S., 1995. Terrestrial ecosystems and the carbon cycle. Glob. Chang. Biol. 1 (1), 77–91. https://doi.org/10.1111/j.1365-2486.1995.tb00008.x.

Schimel, D.S., House, J.I., Hibbard, K.A., Bousquet, P., Ciais, P., Peylin, P., Wirth, C., 2001. Recent patterns and mechanisms of carbon exchange by terrestrial ecosystems. Nature 414 (6860), 169–172. https://doi.org/10.1038/35102500.

Sen, P.K., Lindeman, R.H., Merenda, P.F., Gold, R.Z., 1981. Introduction to bivariate and multivariate analysis. J. Am. Stat. Assoc. 76 (375), 752. https://doi.org/10.2307/2287559.

Steven, C.W., 2001. Climate change enhanced: where has all the carbon gone? Science 292, 2261–2263. https://doi.org/10.1126/science.1061077.

Suchet, P.A., Probst, J.L., 1995. A global model for present-day atmospheric/soil CO_2 consumption by chemical erosion of continental rocks (GEM-CO_2). Tellus B 47 (1–2), 273–280. https://doi.org/10.1034/j.1600-0889.47.issue1.23.x.

Ulrike, G., 2006. Relative importance for linear regression in R: the package relaimpo. J. Stat. Softw. 17, 1–27. https://doi.org/10.18637/jss.v017.i01.

Wan, S., Norby, R.J., Ledford, J., Weltzin, J.F., 2007. Responses of soil respiration to elevated CO_2, air warming, and changing soil water availability in a model old-field grassland. Glob. Chang. Biol. 13 (11), 2411–2424. https://doi.org/10.1111/j.1365-2486.2007.01433.x.

West, A., Galy, A., Bickle, M., 2005. Tectonic and climatic controls on silicate weathering. Earth Planet. Sci. Lett. 235 (1–2), 211–228. https://doi.org/10.1016/j.epsl.2005.03.020.

Xu, G.Q., Liu, Z.Y., Jiang, Z.H., 2006. Decomposition model and empirical study of carbon emissions for China, 1995 - 2004. China Population Resources and Environment 16 (6), 158–161. https://doi.org/10.3969/j.issn.1002-2104.2006.06.030.

Zeng, S., Jiang, Y., Liu, Z., 2016a. Assessment of climate impacts on the karst-related carbon sink in SW China using MPD and GIS. Glob. Planet. Chang. 144, 171–181. https://doi.org/10.1016/j.gloplacha.2016.07.015.

Zeng, C., Liu, Z., Zhao, M., Yang, R., 2016b. Hydrologically-driven variations in the karst-related carbon sink fluxes: insights from high-resolution monitoring of three karst catchments in Southwest China. J. Hydrol. 533, 74–90. https://doi.org/10.1016/j.jhydrol.2015.11.049.

Zhang, J.P., Zhang, L.B., Xu, C., Liu, W.L., Qi, Y., Wo, X., 2014. Vegetation variation of mid-subtropical forest based on MODIS NDVI data—a case study of Jinggangshan City, Jiangxi Province. Acta Ecol. Sin. 34 (1), 7–12. https://doi.org/10.1016/j.chnaes.2013.09.005.

Zhang, L., Qin, X., Liu, P., Huang, Q., 2016. Chemical denudation rate and atmospheric CO_2 consumption by H_2CO_3 and H_2SO_4 in the Yangtze River Catchment. Acta Geol. Sin. 90, 1933–1944. https://doi.org/10.3969/j.issn.0001-5717.2016.08.021.